

THE USE OF THE SINGLE FREQUENCY GPS MEASUREMENTS TO DETERMINE IN REAL TIME ARTIFICIAL SATELLITE ORBITS

Ana Paula Marins Chiaradia*

Hélio Koiti Kuga

Antonio Fernando Bertachini de Almeida Prado

INPE – Instituto Nacional de Pesquisas Espaciais

Av. dos Astronautas, 1758 - Jardim da Granja

São José dos Campos - SP - Brazil - CEP: 12 227-010

*chiara@dem.inpe.br

ABSTRACT

A simple model to determine the orbit of an artificial satellite in real time, using single frequency GPS measurements, is considered. The artificial satellite is above 1000 km of the Earth's surface. The estimation method, in this work, is the extended Kalman filter which is used to estimate in real time the spacecraft's orbit aboard. As the goal of this work is to have relatively standard accuracy (around tens of meters) along with minimum computational cost, the Cowell's method is used to propagate the state vector. The modeled forces are due to the geopotential taking into account the spherical harmonic coefficients up to 50th order and degree of JGM-2 model. To propagate the state covariance matrix, it is considered a more simplified model than the one used in the dynamical model. For computing the state transition matrix, the effect of J_2 is considered. In the measurement model, the single frequency GPS pseudorange is used considering the effects of the ionospheric delay, clock offsets of the GPS and user satellites, and relativistic effects. A dual frequency GPS model is still used to remove them. Several comparisons are made to assess the effects that should be taken into account, as well as to have a trade-off to weigh amongst accuracy, computer load, fastness, and real time constraints. To validate this model, real data are used from Topex/Poseidon satellite which has a dual frequency GPS receiver aboard, and the results are compared with the Topex/Poseidon Precision Orbit Ephemeris (POE) generated by NASA/JPL.

Key words: Kalman filtering, GPS, real time, orbit determination, and single frequency.

INTRODUCTION

The orbit determination process consists of obtaining values of the parameters which completely specify the motion of an orbiting body, like satellite through space, based on a set of observations of the body. It involves system models, measurement model which depends on the tracking system, and estimation technique. One of the big evolutions of this process has been the tracking system.

The observation may be obtained from the ground station networks using laser, radar, Doppler, etc., or by space navigation systems as Transit, Argos, Global Orbiting Navigation Satellite System (GLONASS), Global Positioning System (GPS), and Tracking and Data Relay Satellite System (TDRSS). The choice of the tracking system depends on a compromise between the goals of the mission and the tools available.

In the case of GPS, the advantages are global cover, high precision, low cost and autonomous navigation resources. The GPS may provide orbit determination with accuracy at least as good as methods using ground tracking networks. The latter provides standard precision around hundred meters and the former can provide precision as tight as some centimeters.

The GPS provides, at a given instant, a set of many redundant measurements which makes the orbit position observable geometrically.

With the advances of technology, the single frequency GPS receivers provide a good basis to achieve fair precision at relatively low cost, still

attaining the accuracy requirements of the mission.

GPS SYSTEM

The GPS consists of 24 satellites. The satellites are distributed in six orbital planes inclined at 55°, with a nodal separation of 60°. The orbits are circular with 12 hour period.

Each satellite broadcasts navigation signals on two L band frequencies: 1.57542 GHz (L1) and 1.2276 GHz (L2). The corresponding carrier wavelengths are approximately 19 and 24 cm. The two frequencies are used to calibrate the ionospheric delay.

The GPS allows the receiver to determine its position and time geometrically anywhere at any instant with data from only four satellites. Each satellite broadcast its orbit, its clock offset, and the range measurement between it and the receiver. If the measurements are accurate, a sequentially dynamical orbit determination may not need such a precise force model as the whole information is locally provided by the measurements. This approach was applied in the work of Wu *et al.*²¹, which uses the so-called reduced dynamic technique. Very few experiments were tried using GPS receiver aboard, as Landsat 4, 5, Topex/Poseidon and Extreme Ultraviolet Explorer (EUVE).

SYSTEM MODEL

The system model consists of the description for the dynamics of the orbital motion of a satellite, measurements models, Earth's rotation effects, and perturbation models.

Dynamical Model

The orbits of most of the bodies in space can be described as two-body orbits to some degree of accuracy. However, to achieve better accuracy some perturbations shall be considered, though taking into account the minimum computational cost loads which are one of the goals of this work.

The modeled forces in this work are due to geopotential, taking into account the spherical harmonic coefficients up to 50th order and degree

of JGM-2 model. The integration is carried out by using the simple fourth order Runge-Kutta algorithm without any mechanism of step adjustment or error control. The fourth order Runge Kutta is considered an adequate numerical integrator due to its simplicity, fair accuracy, and low computational burden.

The dynamic equation of motion is given by:

$$\ddot{\mathbf{r}} = -\frac{\mathbf{m}}{r^3}\mathbf{r} + \mathbf{a}_{GEO}, \quad (1)$$

where \mathbf{m} is the geo-gravitational constant, \mathbf{a}_{GEO} is the acceleration due to the perturbing geopotential, computed according to Pines¹⁶. The solar radiation pressure was not considered in this work yet because the results comprised only during two hours, where such effects are not magnified.

Measurement Model

The GPS provides two kinds of measurements: code and carrier phase pseudoranges. Pseudorange is the range between the phase centers of the GPS satellite and receiver antennas, plus the offset between the transmitter and receiver clocks. The pseudorange measurements, however, are corrupted by various error sources. The error sources can steam from three groups: satellite (clock bias, orbital errors), signal propagation (ionospheric and tropospheric refraction), and receiver (antenna phase center variation, clock bias, and multipath). In this work, the considered errors are the GPS satellite and receiver clock bias, and ionospheric refraction. Therefore, the equation of the code pseudorange in L1 frequency is given by:

$$y_c = \mathbf{r}_k + I_k + c[\mathbf{D}t_{sv}(t_k) - \mathbf{D}t_u(t_k)] - \mathbf{e}_k, \quad (2)$$

where y_c is the code pseudorange in L1, I_k is the ionospheric delay, c is the vacuum speed of light, $\mathbf{D}t_{sv}(t_k)$ is the GPS satellite clock offset, $\mathbf{D}t_u(t_k)$ is the receiver clock offset, t_k is the observation instant in GPS time, \mathbf{r}_k is the geometric range given by:

$$\mathbf{r} = \sqrt{(x_{GPS} - x)^2 + (y_{GPS} - y)^2 + (z_{GPS} - z)^2}, \quad (3)$$

x , y , and z are the positional states of the user satellite at the reception time, x_{GPS} , y_{GPS} , and z_{GPS} are the positional states of the GPS satellite at the transmission time (corrected for light time delay), and e_k is a remnant error supposed random gaussian.

Study of the Ionospheric Correction Model

When the signals are transmitted from the GPS satellite to the receiver, they propagate through the ionosphere causing errors on the measurements which are the highest ones on the signal propagation. To analyze the effect of this error, some models as Klobuchar's, Dual frequency, and Empirical, have been studied considering a user above 1000 km of the Earth's surface.

The Klobuchar's model is used to correct the ionospheric effect for single frequency measurements. It uses the cosine model for a daily variation of the ionosphere with the maximum being at 14:00hs local time. It is described by 8 coefficients α and β which are transmitted as part of the GPS satellite navigation message. This model removes about 50% of the total ionospheric delay at mid-latitudes, being necessary to use an estimation model to evaluate the remaining unmodeled errors, and it is represented through one set of the variables that are valid for few days. It must be used for a user on the Earth's surface. Therefore, this model can not be used in this work. For more details, see Klobuchar⁷.

The empirical model of the Earth's plasmasphere consists of an analytical expression that can be used to reproduce hydrogen density at arbitrary locations in the plasmasphere for given conditions. The main spatial dependence of plasmaspheric electron density is governed by the L-shell. The L-shell is the surface traced out by a particle moving around the Earth's geomagnetic field lines. It is a good choice for a user above 1000 km, despite this algorithm does not model diurnal, seasonal, or solar cycle variations of the plasmaspheric electron content. For more details, see Gallagher *et. al.*⁵. For more details about the ionospheric correction model, see Komjathy⁸.

The secondary frequency L2 was incorporated into the system to allow users to automatically correct the effects of both the range and range rate errors induced by the ionosphere. The dual frequency GPS receivers take advantage of the dispersive nature of the ionosphere and can eliminate (to first order) the ionospheric errors. This model is used to analyze this effect and to verify if it is necessary to use some other model. In this case, it is possible because the tested satellite has a dual frequency receiver aboard. The expression for the corrected code pseudorange measurement are given by:

$$y_{IF} = \frac{f_1^2}{f_1^2 - f_2^2} y_1 - \frac{f_2^2}{f_1^2 - f_2^2} y_2, \quad (4)$$

where y_{IF} is the free code pseudorange of the ionospheric effect, y_1 and y_2 are the code pseudorange measurements in L1 and L2, respectively, f_1 is the frequency in L1, and f_2 is the frequency in L2.

The Figure 1 shows the ionospheric errors of the code pseudorange measurements for one day.

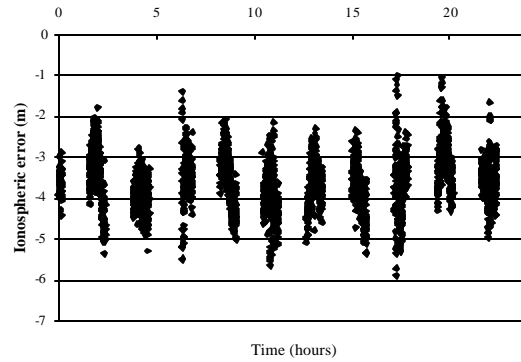


Figure 1: The code pseudorange ionospheric error

The average ionospheric effect for one day is - 3.62 m. If the goal of this work were accuracy better than meters, the ionospheric effect must be considered in the model and, in this case, a ionospheric correction model for single frequency must be used. In spite of this, the dual frequency model is used to correct it².

As developed by Goad⁶, if the carrier phase is incorporated to the model, the ambiguity (number

of the cycles) and the ionospheric effects can be estimated jointly as part of the state using some estimation procedure as the Kalman filtering, since observability conditions are provided.

Clock Error Terms

The third term of the right-side of the equation (2) is the clock bias which represents the combined clock offsets of the satellite and of the receiver with respect to the GPS time. Each GPS satellite contributes with one clock bias. The information for the GPS satellite clocks is known and transmitted via the broadcast navigation message in the form of three polynomial coefficients with a reference time t_{oc} . The clock correction of the GPS satellite for the epoch t is²⁰:

$$t = t_{sv} - \mathbf{D}t_{sv} \quad (5)$$

where

$$\mathbf{D}_{sv} = a_{f0} + a_{f1}(t - t_{oc}) + a_{f2}(t - t_{oc})^2 + \mathbf{D}_R, \quad (6)$$

and

$$\mathbf{D}t_R = -\frac{2}{c^2} \sqrt{a m e \sin E}, \quad (7)$$

where t is the GPS time in seconds, t_{sv} is the spacecraft code phase time at message transmission time in seconds, t_{oc} is the reference time in seconds, measured from the GPS time weekly epoch, a_{f0} , a_{f1} , and a_{f2} are parameters, $\mathbf{D}t_R$ is a small relativistic clock correction caused by the orbital eccentricity, e is the eccentricity, a is the semi-major axis of the orbit, and E is the eccentric anomaly. The polynomial coefficients a_{f0} , a_{f1} , and a_{f2} are transmitted in units of sec, sec/sec, and sec/sec², respectively. The clock data reference time t_{oc} is also broadcast. The value of t_{sv} must account for the beginning or the end-of-week crossovers. The user may approximate t by t_{sv} in the equation (6)²⁰. The user clock offset is part of the estimated state vector as¹⁸:

$$c\mathbf{D}_u = b + \dot{b}\mathbf{D} + \ddot{b}\mathbf{D}^2 \quad (8)$$

where b is the receiver clock bias, \dot{b} is the drift, \ddot{b} is the drift rate and Δt is the elapsed time of measurements.

ESTIMATION TECHNIQUE

The orbit determination problem, which has a non-linear dynamical system and a non-linear measurement system, can be formulated in a way that make it possible to apply one of the best known methods of sequential linear estimation, the Kalman Filter.

The extended Kalman filter is a Kalman filter version applicable to problems like this one, composed by a time-updated and a measurement-updated cycles. The time-updated phase updates the state and the covariance matrix along the time using the dynamical equations.

In this work, a simple reduced state vector is chosen to be estimated:

$$\mathbf{x} = (\mathbf{r}, \mathbf{v}, b, \dot{b}, \ddot{b})^T, \quad (9)$$

where $\mathbf{r} = (x, y, z)^T$ and $\mathbf{v} = (\dot{x}, \dot{y}, \dot{z})^T$ are the spacecraft's position and velocity vector, b is the receiver clock bias, \dot{b} is the drift, and \ddot{b} is the drift rate.

Then, the differential dynamic equations of motion to be integrated are given by:

$$\dot{\mathbf{x}} = \mathbf{f}(\mathbf{x}, t), \quad (10)$$

and

$$\dot{\mathbf{F}} = \mathbf{F}\mathbf{F}, \quad (11)$$

where $\mathbf{f}(\mathbf{x}, t)$ is the vector-valued function of time and the state, \mathbf{F} is the state transition matrix which relates the state between t_k and t_{k+1} , and $\mathbf{F} = \partial \mathbf{f}(\mathbf{x}, t) / \partial \mathbf{x}$.

Both equations should be numerically integrated simultaneously, so that \mathbf{F} is evaluated always along the most current state \mathbf{x} . Next, one updates the covariance matrix \mathbf{P} by means of the discrete Riccati equation:

$$\bar{\mathbf{P}}_{k+1} = \mathbf{F}_{k+1} \hat{\mathbf{P}}_k \mathbf{F}_{k+1}^T + \mathbf{Q}_k, \quad (12)$$

where \hat{P}_k is the covariance matrix after processing all measurements at time t_k , F is the state transition matrix obtained by the previous integration and Q_k is the discrete state-noise covariance which is a measurement of the error between the reference state and the true state arising from imperfect modeling. The P_k matrix is a measurement of accuracy of the errors knowledge.

At the end of this process, \bar{x}_{k+1} and \bar{P}_{k+1} , are obtained and are called time-updated state and covariance, respectively.

The measurement residual and the sensitivity matrix are found by forming the computed observation equation. The model for the GPS pseudorange measurement is given by the equation (2).

The sensitivity matrix is given by:

$$H_k = \begin{bmatrix} -\frac{(x_{GPS} - x)}{r}, -\frac{(y_{GPS} - y)}{r}, -\frac{(z_{GPS} - z)}{r}, \\ 0, 0, 0, 1, Dt, Dt^2 \end{bmatrix}, \quad (13)$$

where Dt is the elapsed time of measurements.

The measurement residual, or innovation sequence is:

$$y_k = Y_k - y_c(\mathbf{x}_k, t_k), \quad (14)$$

where Y_k is the observed measurement and y_c is the calculated measurement by the equation (2).

The measurement updated phase uses the Kalman equations to incorporate the information given by the measurements themselves, and obtains improved estimates of the state and of the covariance:

$$K_k = \bar{P}_k H_k^T (H_k \bar{P}_k H_k^T + R_k)^{-1}, \quad (14)$$

$$\hat{x}_k = \bar{x}_k + K_k y_k, \quad (15)$$

$$\hat{P}_k = (I - K_k H_k) \bar{P}_k, \quad (16)$$

where R_k is the discrete measurement noise covariance, which is basically a measurement weight matrix. These equations can be used to process the measurements sequentially so that the matrix inversion in (14) is a scalar. To be precise, the measurements should be uncorrelated, in which case the measurement covariance noise R_k is diagonal.

TRANSITION MATRIX

The function of the transition matrix is to relate the state errors between t_k and t_{k+1} times. Binning¹ has suggested one method to avoid the problem of the high computational cost and extended analytical expressions of the transition matrix. This method consists of propagating the state vector using complete force model and, then, to compute the transition matrix using a simplified force model. The proposed method is used in this work and the transition matrix is propagated by the Markley's method¹³.

The Markley's method uses two states, one in t_{k-1} time and other in t_k time, and calculates the transition matrix between them using m , J_2 , Dt , the radius of the Earth, and the two states. In this case, the effect of Earth flattening is the most influent factor in the process^{9,14}.

The Markley's method consists of making one approximation to the transition matrix of the state vector based on Taylor series expansion for short intervals of propagation, Dt . However, this method is used only to propagate the position and velocity of the user.

The state transition's differential equation is defined as:

$$\frac{d\mathbf{f}(t, t_0)}{dt} = A_f(t) \mathbf{f}(t, t_0) = \begin{bmatrix} 0 & I \\ G(t) & 0 \end{bmatrix} \mathbf{f}(t, t_0) \quad (17)$$

where $\mathbf{F}(t_0, t_0) \equiv \mathbf{I}$ is the initial condition,

$$\mathbf{f}(t, t_0) = \begin{bmatrix} \frac{\partial \mathbf{r}}{\partial \mathbf{r}_0} & \frac{\partial \mathbf{r}}{\partial \mathbf{v}_0} \\ \frac{\partial \mathbf{v}}{\partial \mathbf{r}_0} & \frac{\partial \mathbf{v}}{\partial \mathbf{v}_0} \end{bmatrix} \quad (18)$$

where $\mathbf{r} = (x \ y \ z)^T$ and $\mathbf{v} = (\dot{x} \ \dot{y} \ \dot{z})^T$ are the Cartesian state at the instant t , \mathbf{r}_0 and \mathbf{v}_0 are the Cartesian state in t_0 , $\mathbf{0} \equiv$ matrix 3x3 of zeros, $I \equiv$ identity matrix 3x3, $G(t) \equiv \frac{\partial \mathbf{f}(\mathbf{r}, t)}{\partial \mathbf{r}} \equiv$ gradient matrix e $\mathbf{f}(\mathbf{r}, t) =$ accelerations on the satellite.

Developing the Markley's method, the transition matrix for position and velocity is given by:

$$\mathbf{F}(t, t_0) \approx \begin{bmatrix} \mathbf{F}_{rr} & \mathbf{F}_{rv} \\ \mathbf{F}_{vr} & \mathbf{F}_{vv} \end{bmatrix}_{6 \times 6} \quad (19)$$

where

$$\begin{aligned} \mathbf{F}_{rr} &\equiv I + (2G_0 + G) \frac{(\mathbf{D}t)^2}{6}, \\ \mathbf{F}_{rv} &\equiv I \mathbf{D}t + (G_0 + G) \frac{(\mathbf{D}t)^3}{12}, \\ \mathbf{F}_{vr} &\equiv (G_0 + G) \frac{(\mathbf{D}t)}{2}, \\ \mathbf{F}_{vv} &\equiv I + (G_0 + 2G) \frac{(\mathbf{D}t)^2}{6}. \end{aligned} \quad (20)$$

where $\mathbf{D}t \circ t_k - t_0$ and $G_0 \circ G(t_0)$.

The G and, therefore, $\mathbf{F}_{rr}, \mathbf{F}_{rv}, \mathbf{F}_{vr}, \mathbf{F}_{vv}$ are symmetric if the perturbation is derived from potential. The G gradient matrix, including only the central force and the J_2 , is given by:

$$G(t_k) = \frac{\partial \mathbf{f}(\mathbf{r}, t_k)}{\partial \mathbf{r}} = \begin{bmatrix} \frac{\partial f_x}{\partial x} & \frac{\partial f_x}{\partial y} & \frac{\partial f_x}{\partial z} \\ \frac{\partial f_y}{\partial x} & \frac{\partial f_y}{\partial y} & \frac{\partial f_y}{\partial z} \\ \frac{\partial f_z}{\partial x} & \frac{\partial f_z}{\partial y} & \frac{\partial f_z}{\partial z} \end{bmatrix}. \quad (21)$$

The accelerations due to Earth flattening are given by:

$$f_x = \frac{-\mathbf{m}\kappa}{r^3} \left[1 + \frac{3}{2} \frac{J_2 R_e^2}{r^2} \left(1 - \frac{5z^2}{r^2} \right) \right],$$

$$f_y = \frac{y}{x} f_x,$$

$$f_z = \frac{-\mathbf{m}\kappa}{r^3} \left[1 + \frac{3}{2} \frac{J_2 R_e^2}{r^2} \left(3 - \frac{5z^2}{r^2} \right) \right]. \quad (22)$$

The partial derivatives are¹²:

$$\begin{aligned} \frac{\partial f_x}{\partial x} &= \frac{\mathbf{m}}{r^5} \left[3x^2 - r^2 - \frac{3}{2} J_2 R_e^2 + \frac{15}{2} \frac{J_2 R_e^2}{r^2} (x^2 + z^2) \right. \\ &\quad \left. - \frac{105}{2} \frac{J_2 R_e^2}{r^4} x^2 z^2 \right], \\ \frac{\partial f_x}{\partial y} &= \frac{3\mathbf{m}\kappa y}{r^5} \left[1 + \frac{5}{2} \frac{J_2 R_e^2}{r^2} - \frac{35}{2} \frac{J_2 R_e^2}{r^4} z^2 \right], \\ \frac{\partial f_x}{\partial z} &= \frac{3\mathbf{m}\kappa z}{r^5} \left[1 + \frac{15}{2} \frac{J_2 R_e^2}{r^2} - \frac{35}{2} \frac{J_2 R_e^2}{r^4} z^2 \right]. \end{aligned} \quad (23)$$

The transition sub-matrix for clock bias, clock drift, and drift rate is given by:

$$\mathbf{F}(t, t_0) = \begin{bmatrix} 1 & 0 & 0 \\ 0 & 1 & 0 \\ 0 & 0 & 1 \end{bmatrix}. \quad (24)$$

DATA SET

To analyze the proposed method, the Topex/Poseidon satellite (T/P) data is chosen because it carries a dual frequency receiver GPS aboard experimentally to test the ability of the GPS to provide precise orbit determination (POD). The observation data T/P GPS data set and navigation message in Rinex format are easily found in the Internet^{15,19}.

As suggested by Binning¹, one uses the T/P data set of November 18th, 1993, because Selective Availability (SA) was also not in operation for 18 (2 Block I [PRNs 3, 13], 6 Block II [PRNs 14, 15, 16, 17, 20, 21], 10 Block II-A [PRNs 1, 5, 7, 9, 22, 23, 2, 26, 28, 31]) of the 25 available GPS satellites allowing civilian users access to the most precise GPS measurements. At that time,

the GPS constellation was not yet considered fully operational, and therefore, Anti-Spoofing was also off. This allowed all users to receive clean data in both L1 and L2 frequencies.

The position and velocity estimated in this work are compared against the TOPEX/Poseidon Precise Orbit Ephemeris (POE)¹⁹ generated by the Jet Propulsion Laboratory (JPL) in UTC time. The JPL/POE is claimed to estimate T/P position to an accuracy of better than 15 cm (See Ref. 1 for details). The states in the POE are provided in one minute UTC time steps in Inertial True of Date coordinates. But, the T/P GPS measurements are provided in 10 seconds of GPS time. Accordingly to IERS, the difference between the UTC and GPS time is 9 seconds at this date. Therefore, it was necessary to interpolate the states in one second steps through the ODEM Orbit Determination software^{10,11}.

TOPEX/Poseidon satellite

The mission is jointly conducted by the United States National Aeronautics and Space Administration (NASA) and the French space agency, Centre National d'Etudes Spatiales (CNES). The main goal of this mission is to improve the knowledge of the global ocean circulation. Other applications include the ocean tides, geodesy and geodynamics, ocean wave height, and wind speed⁴.

The T/P spacecraft orbits the Earth at an altitude of 1336 km, inclination of 66° and with nearly zero eccentricity. The period of the orbit is 1.87 hours.

This satellite carries a total of five tracking systems including Satellite Laser Ranging (SLR), DORIS Doppler, GPS, TDRSS, and the satellite altimeter itself. The satellite orbit must be determined with a RMS radial accuracy of 13 centimeters. This is an extremely stringent accuracy requirement for a satellite of this shape and altitude¹⁷.

The T/P receiver can track up to 6 GPS satellites at once on both frequencies if Anti-Spoofing is inactive².

RESULTS

In accordance with studies done previously³, good results are obtained considering one simplified dynamical model where the modeled forces are geopotential up to 23rd order and degree of the spherical harmonic coefficients and a simplified model can be considered to propagate the state covariance matrix. In this study, it has been checked that 10-second step-size to be used in the numerical integrator provides good results at minimum computational cost as outlined in this work. However, the measurement model shall be carefully modeled as some effects can be very pronounced.

Aiming at improving this model, new tests were carried out. One of them is concerned with the modeled forces. It is verified that the 50th order and degree of the spherical harmonic coefficients can provide the results without raising the computational cost. Other tests developed are concerned with the ionospheric and SA effects, and the transition matrix. Additionally, it is analyzed the GPS ephemeris software which results are presented here.

According to Chiaradia³, the ionospheric effect is one of the smallest errors among the considered effects in the measurement model cited previously. The Figures 2 and 3 show the error caused by the ionospheric effect on the orbit determination of an artificial satellite above 1000 km, in this specific case, the T/P satellite. The Table 1 shows the statistical errors for this case where s is the standard deviation. All tests are compared with the full model for a span of two hours. The full model consists of the measurement model cited in the equation (2), the ionospheric correction, the effect of the J2 considered in the transition matrix, SA off, and the 50th order and degree of the spherical harmonic coefficients of JGM-2 model.

To analyze the transition matrix considering the effect of J₂ on the orbit determination, it is developed one comparison between the estimated orbits with the effect of J₂ and a pure Keplerian model in the transition matrix. The Figures 4 and 5 show the difference between the estimated orbits caused by the transition matrix. The Table 3 show the statistical errors for transition matrix in the estimated orbit.

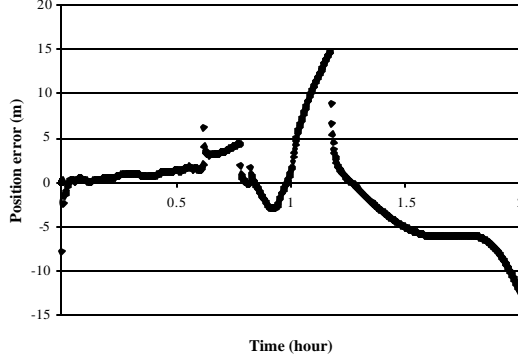


Figure 2: Position error due to ionospheric effect.

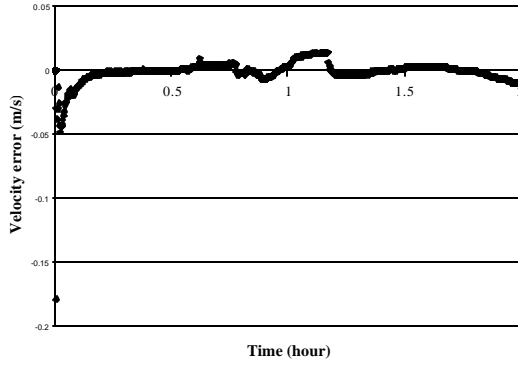


Figure 3: Velocity error due to ionospheric effect

Table 1: Statistical error for ionospheric effect.

	Position (m)	Velocity (m/s)
error mean	-0.0075	-1.31×10^{-5}
error s	0.52	0.0011
Max. error	14.805	0.014
Min. error	-12.299	-0.179

To analyze the effect of the SA in the estimated orbit, the following test is developed. First, the estimated orbit considers the GPS satellites with SA on and, next, with SA off. One notes that the results with SA on is better than with SA off as cited in Binning¹. The Figure 6 shows the code pseudorange residual corrupted with SA. The average number of satellites being tracked by the T/P receiver on this epoch during two hours is 5.54 and the average number of used GPS satellites (not rejected) is 3.76. However, when

the SA corrupted satellites are removed the average drops to 2.69.

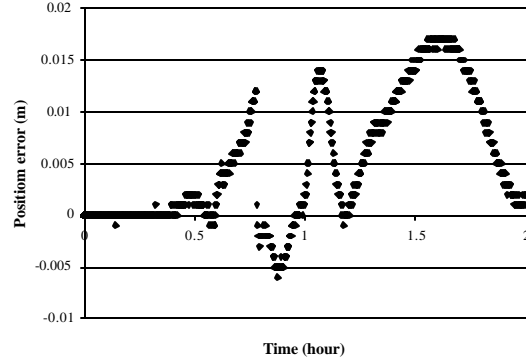


Figure 4: Position error due to the transition Matrix

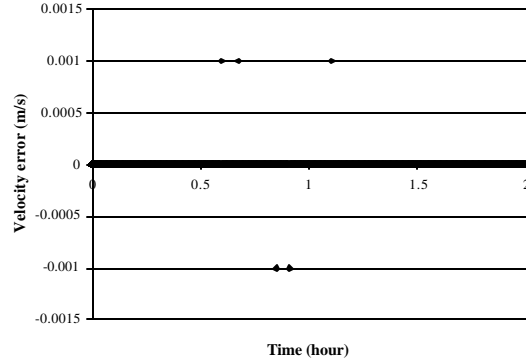


Figure 5: Velocity error due to the transition Matrix

Table 2: Statistical error for transition matrix.

	Position (m)	Velocity (m/s)
error mean	5.675×10^{-5}	1.526×10^{-8}
error s	8.4×10^{-4}	8.735×10^{-6}
Max. error	0.017	0.001
Min. error	-0.006	-0.001

The Figures 7 and 8 show the position and velocity error, respectively, compared with the JPL/POE. The Table 3 shows the statistical errors.

To analyze the effect of the error caused by the GPS ephemeris computed through the navigation message, it is compared such ephemeris with post-processed GPS ephemeris (POE) generated by JPL¹⁵. The Figure 9 shows the error between them for each satellite during two hours.

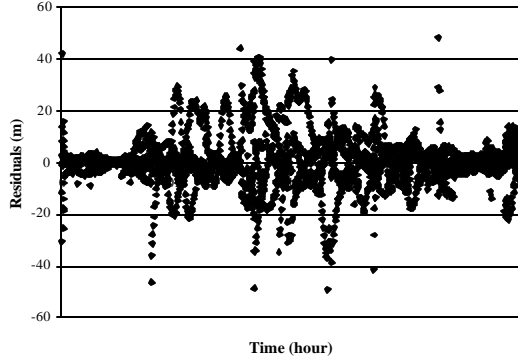


Figure 6: The code pseudorange residual corrupted with SA.

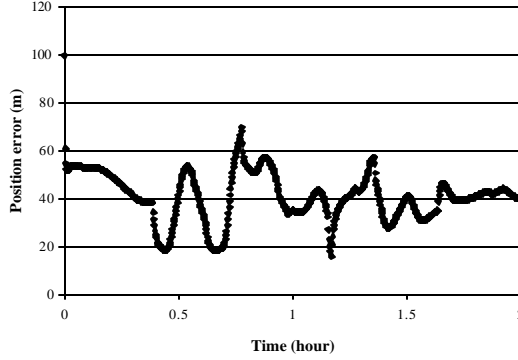


Figure 7: The position error

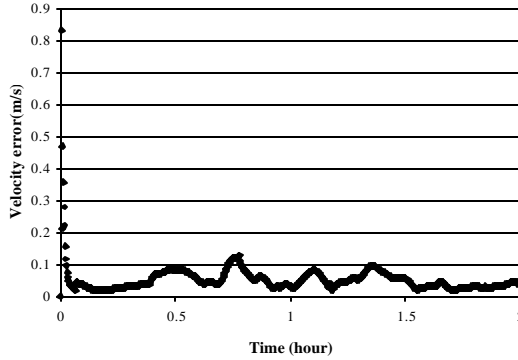


Figure 8: The velocity error

Table 3: The statistical error for position and velocity.

	Position (m)	Velocity (m/s)
error mean	41.07	0.053
s	10.2381	0.044
RMS	42.338	0.069

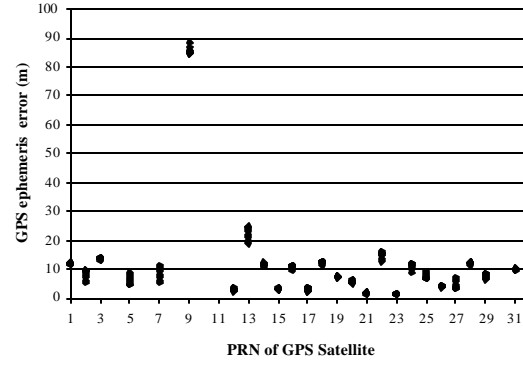


Figure 9: The error of the GPS ephemeris calculated by navigation message.

The Table 4 shows the comparative statistics between the GPS ephemeris calculated by our software and JPL.

Table 4: Statistical error of the GPS ephemeris.

error mean	11.6 m
error s	15.91 m
Max. error	88.5073 m
Min. error	1.17414 m

CONCLUSIONS

The main goal of this work was to achieve accuracy around tens of meters when determining in real time the artificial satellite orbits considering a simplified model. To develop it, the single frequency GPS measurements are used.

With respect of the dynamical model, the 50th order and degree of the spherical harmonic coefficients provide good results without raising the computational cost. However, a truncation to the 23rd order and degree still can be used providing acceptable accuracy. The solar radiation pressure shall be considered in tests of long period.

With respect to the measurement model, the ionospheric effect can be neglected or jointly estimated as part of the state for satellites above 1000 km of the Earth's surface when the requirement of the mission is accuracy around tens of meters.

The transition matrix considering the effect of J_2 do not provide reasonable improvements in the

estimated orbit despite having low computational cost.

The removal of the GPS satellites with SA on do not provide good results for the sampled data. Other tests using different data shall be conducted to investigate the contradictions.

The GPS ephemeris generated by our software is calculated with good accuracy without affecting the estimated orbit.

ACKNOWLEDGEMENT

The authors wish to express their appreciation for the support provided by CAPES (*Fundação para Coordenação de Aperfeiçoamento de Pessoal de Nível Superior*) - Brazil and INPE (Brazilian Institute for Space Research) - Brazil.

REFERENCES

- ¹Binning, P. W. *Absolute and Relative Satellite To Satellite Navigation using GPS*. Ph.D. Dissertation. Department of Aerospace Engineering Sciences. University of Colorado. 1997.
- ²Chiaradia, A. P. M.; Kuga, H. K.; Prado, A. F. B.A. Investigation on the GPS signal ionospheric correction. Presented in *IX Brazilian Orbital Dynamics Colloquium*, Águas de Lindóia - SP - Brazil, November, 1998.
- ³Chiaradia, A. P. M.; Kuga, H. K.; Prado, A. F. B.A. Investigation of simplified models for orbit determination using single frequency GPS measurements. Presented in *14th International Symposium on Space Flight Dynamics*, Foz de Iguaçu - PR - Brazil, February, 1999.
- ⁴Fu, L. L.; Christensen, E. J.; Yamarone Jr., C. A. TOPEX/POSEIDON mission overview. *Journal of Geophysical Research*, Vol. 99, N. C12, p24369-24381, December 15, 1994.
- ⁵Gallagher, D. L.; Craven, P. D.; Comfort, R. A. An Empirical Model of the Earth's Plasmasphere. *Adv. Space. Res.* Vol. 8, N. 8, p(8)15-(8)24, 1988.
- ⁶Goad, C. C. Optimal Filtering of Pseudoranges and Phases from Single-Frequency GPS receivers. *Navigation: Journal of the Institute of Navigation*. Vol. 37, N. 3, Fall, 1990.
- ⁷Klobuchar, J. A. Ionospheric Time-Delay Algorithm for Single-Frequency GPS users. *IEEE Trans. on Aerospace and Elec. Systems*. Vol. AES-23, N. 3, May, 1987.
- ⁸Komjathy, A. *Global Ionospheric Total Electron Content Mapping Using Global Positioning System*. Ph.D. Dissertation, Department of Geodesy and Geomatics Engineering Technical Report N. 188, University of New Brunswick, Fredericton, New Brunswick, Canada, 248p. 1997.
- ⁹Kuga, H. K. *Determinação de órbitas de satélites artificiais terrestres através de técnicas de estimação combinadas a técnicas de suavização de estado*. INPE - São José dos Campos - SP, 249p. (INPE-4959-TDL/079). Ph.D. Dissertation. 1989. (in Portuguese).
- ¹⁰Kuga, H. K.; Gill, E. A *Mathematical Description of the ODEM Orbit Determination Software*. DLR-GSOC-IB-94-06, DLR, 1994.
- ¹¹Kuga, H. K.; Gill, E.; Montenbruck, O. Orbit Determination and Apogee Boost Maneuver Estimation Using UD-filtering. DLR-GSOC IB 91-2, DLR, 1991.
- ¹²Kuga, H.K. Estimação adaptativa de órbitas aplicada a satélites a baixa altitude. *Master Thesis*, INPE, São José dos Campos, INPE-2316-TDL/079, 1982. (in portuguese).
- ¹³Markley, F. L. Approximate Cartesian State Transition Matrix. *The Journal of the Astronautical Sciences*. Vol. 34, n. 2, p161-169, abril-junho, 1986.
- ¹⁴May, J.A. A study of the effects of state transition matrix approximations. *Proceedings, Flight Mechanics/ estimation theory Symposium*, Greenbelt, MA, p29-48, 1979.
- ¹⁵Noll, C. *Crustal Dynamics Data Information System*. [On-line] <ftp://cddisa.gsfc.nasa.gov/>, Dec., 1998.

¹⁶Pines, S. Uniform representation of the gravitational potential and its derivatives. *AIAA Journal*, Vol.11, No.11, Nov., 1973.

¹⁷Putney, B. H.; Marshall, J. A.; Nerem, R. S.; Lerch, F. J.; Chinn, D. S.; Johnson, C. C.; Klosko, S. M.; Luthcke, S. B.; Rachlin, K. E.; Williams, T. A.; Williamson, R. G.; Zelensky, N. P. Precise Orbit Determination for the Topex/Poseidon Mission. AAS 93-577. 1993.

¹⁸Seeber, G. *Satellite Geodesy: Foundations, Methods, and Applications*. Walter de Gruyter, Berlin-New York, 1993.

¹⁹Shapiro, B. R. *Topex/Poseidon Navigation Team*. [On-line] <http://topexnav.jpl.nasa.gov>, April, 1998.

²⁰Van Dierendonck, A. J.; Russell, S.S.; Kopitzke, E. R.; Birnbaum, M. The GPS Navigation Message. *Navigation*, Vol. I, p55-73. 1980.

²¹Wu, S.C.; Yunck, T. P.; Thornton, C. L. Reduced dynamic technique for precise orbit determination of low Earth satellites. *J. Guidance, Control and Dynamics*, Vol. 14, pp. 24-30, 1991.